

ADeADA: Adaptive Density-aware Active Domain Adaptation for Semantic Segmentation

Tsung-Han Wu¹ Yi-Syuan Liou¹ Shao-Ji Yuan¹ Hsin-Ying Lee¹ Tung-I Chen¹ Winston H. Hsu^{1,2}

¹National Taiwan University

²Mobile Drive Technology

Abstract

In the field of domain adaptation, a trade-off exists between the model performance and the number of target domain annotations. Active learning, maximizing model performance with few informative labeled data, comes in handy for such a scenario. In this work, we present **ADeADA**, a general active domain adaptation framework for semantic segmentation. To adapt the model to the target domain with minimum queried labels, we propose acquiring labels of the samples with high probability density in the target domain yet with low probability density in the source domain, complementary to the existing source domain labeled data. To further facilitate the label efficiency, we design an adaptive budget allocation policy, which dynamically balances the labeling budgets among different categories as well as between density-aware and uncertainty-based methods. Extensive experiments show that our method outperforms existing active learning and domain adaptation baselines on two benchmarks, *GTA5* \rightarrow *Cityscapes* and *SYNTHIA* \rightarrow *Cityscapes*. With less than 5% target domain annotations, our method reaches comparable results with that of full supervision.

1. Introduction

Semantic segmentation is vital for many intelligent systems, such as self-driving cars and robotics. Over the past ten years, supervised deep learning methods [5–8, 20, 39, 43, 49, 51] have achieved great success assisted by rich labeled datasets. However, obtaining large-scale datasets with manual pixel-by-pixel annotation is still costly in terms of time and effort. Thus, several prior works utilized *domain adaptation* techniques to transfer the knowledge learned from the whole labeled source domain, such as simulated game environments, to real-world unlabeled target domain.

In the field of domain adaptation, a trade-off exists between model performance and the amount of target domain annotations. With sufficient target domain manual

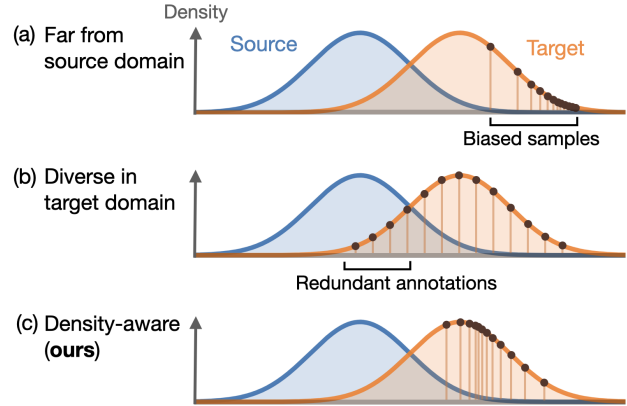


Figure 1. **Different Active Domain Adaptation (ADA) Strategies.** (a) [38, 52] proposed ADA strategies that acquire labels of target samples that are far from the source domain by the trained domain discriminator. However, the selected biased samples are inconsistent with real target distribution. (b) [12, 28, 37] proposed selecting diverse samples in the target domain with clustering techniques for label acquisition. Nonetheless, redundant annotations exist on samples that are similar to the existing labeled source domain dataset. (c) We propose a **density-aware** ADA strategy that acquires labels for samples that are representative in the target domain yet scarce the source domain, which is better than only considering either the source domain (a) or the target domain (b).

annotations, supervised learning method can reach high performance (e.g. 71.3 mIoU on Cityscapes shown in Table 1), while without any target labeling, the performance of unsupervised domain adaptation (UDA) methods [4, 11, 18, 21, 23, 35, 40, 41, 48, 50, 53, 54] are still far below that of full supervision (e.g. 57.5 mIoU on GTA [29] \rightarrow Cityscapes [10] reported by [50]). Compared to the above two extreme cases, which are impractical in real-world applications, a more reasonable manner is to strike a balance between model performance and the cost of labeling efforts.

Active learning, maximizing model performance with few informative labeled data, comes in handy for such a scenario. In the past few years, several works utilized

model uncertainty [13, 31, 34, 36, 42, 44] or data diversity [2, 19, 25, 32, 46] as the indicator to select valuable samples for label acquisition. The core concept of *uncertainty-based methods* is to acquire labels for data close to the model decision boundary, and the main idea of *data diversity approaches* is to query labels for a batch of samples that are far away from each other in the feature space. Recently, some studies proposed active learning methods for domain adaptation, named Active Domain Adaptation (ADA), considering both model uncertainty and data diversity. [38, 52] used the trained classifier and domain discriminator to select highly uncertain samples that are far from the source domain distribution. [12, 28, 37] utilized clustering techniques to select highly uncertain samples that are diverse in target domain distribution.

However, these previous works have two significant defects. To begin with, existing exploration techniques, either selecting samples far from the source domain or diverse in the target domain, is not efficient. As shown in Figure 1, selecting samples far from the source domain might lead to biased data (a), while labeling diverse data in the target domain might cause redundant (b). Moreover, the prior budget allocation policies, relying on uncertainty and diversity equally over time, is not productive. For example, as shown in Figure 2, the uncertainty criterion might fail to detect high-confident error regions in the early stages (a, b, c). Conversely, its advantages is capturing the low-confident error with an accurate model in later stages (d, e, f).

To address the two problems, we present an **Adaptive Density-aware Active Domain Adaptation (ADeADA)** framework for semantic segmentation. For the first issue, we propose a novel *density-aware selection method* to conquer the huge domain gaps between the source and target domain with least acquired annotations. The term “domain density” in this paper describes the prevalence of an observed sample in a specific domain in a high-level view. As our intuition illustrated in Figure 1 (c), since the model have already performed well on source domain data, only a small amount of labeled samples with high target domain density but low source domain density is sufficient for models to overcome domain shift. In addition to experimental supports, our method is also mathematically proved to reduce the generalization bound of domain adaptation.

For the second issue, we develop an *adaptive budget allocation policy* to facilitate the label efficiency. Considering different adaptation difficulties among classes, the *category-balanced selection* provides more budgets on poorly-aligned categories than well-aligned ones in our density-aware method. Additionally, an *dynamic scheduling policy* is designed to balance the budget between the density-aware and uncertainty-based methods over time; thus, we can benefit from the advantages of both and avoid their weaknesses. Since the key idea of the density-aware

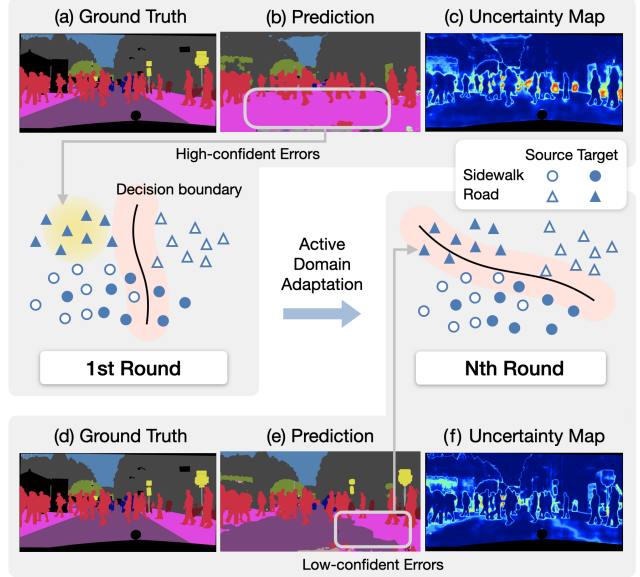


Figure 2. **Adaptive Budget Decision in Active Domain Adaptation (ADA)**. Uncertainty-based active learning methods acquire labels of data close to the decision boundary (red background). Since its inability to detect high-confident error under severe domain shift, several representative samples in the target domain far from the decision boundary will not be selected (yellow background) in early stages, resulting in low label efficiency as shown in (a, b, c). However, as the two domains gradually align by fine-tuning with acquired labels, uncertainty-based method can improve the performance by capturing the low-confident error with an accurate model in later stages, as shown in (d, e, f). As a result, we propose an adaptive budget allocation policy to adjust our selection strategy in the ADA process dynamically (Sec. 3.3.2).

method is to reduce the domain gap, it greatly improves the performance in the early stages when the domain gaps are large but is less effective in the later stage when the two domains are almost aligned as shown in Table 2. In contrast, as discussed in Figure 2, the strength of uncertainty is in later stages, while its defect is in the early stages. Based on these analysis, the scheduling technique is designed to allocate more labeling budgets for density selection in the early stage and more for uncertainty selection in the late stages.

Experimental results demonstrated that our proposed ADeADA surpasses existing active learning and domain adaptation baselines on two widely used benchmarks, GTA5 \rightarrow Cityscapes and SYNTHIA \rightarrow Cityscapes. Moreover, with less than 5% target domain annotations, our method reaches comparable results with full supervision.

To sum up, our contributions are highlighted as follows,

- We open up a new way for ADA that utilizes domain density as an active selection criterion.
- We design an adaptive budget allocation policy to balance the labeling budget among categories and be-

tween active learning methods.

- Extensive experiments demonstrate our method outperforms current state-of-the-art active learning and domain adaptation methods.

2. Related Work

We introduce domain adaptation methods for semantic segmentation with none or few target labels and briefly review the progress of deep active learning.

Unsupervised Domain Adaptation for Semantic Segmentation. Many researchers have delved into unsupervised domain adaptation (UDA) methods for semantic segmentation. One widely-used approach is to align the distribution of the source and target domain through adversarial training [4, 11, 21, 40, 41]. Another popular method is to leverage the self-training technique [50, 53, 54] by assigning pseudo labels to target domain data. However, the performance of distribution alignment is still not satisfying [25], and self-training often suffers from label noise [50]. These defects make existing UDA methods hard to reach the performance of full supervision on labeled target domain data.

Domain Adaptation for Semantic Segmentation with Few Target Labels. To reduce the performance gap between UDA methods and supervision on the whole labeled target domain data, some recent works have explored the utilization of weak and few target domain annotations.

[26] introduced a weakly-supervised domain adaptation (WDA) framework for semantic segmentation, where image-level annotations are provided initially, and few manual or pseudo pixel-level labels are gradually added.

Some considered the semi-supervised domain adaptation (SSDA) scenario, where only a small portion of pixel-level annotations are available during training. [45] attempted to align the features of the source and target domain globally and semantically. [9] reduced the domain shift by mixing domains and knowledge distillation.

Unlike the above settings, where few labels were initially given, others leveraged active learning strategies to gradually query few target annotations from humans. For example, [25] chose diverse target domain images dissimilar to multiple source domain anchors for labeling. [34] utilized the inconsistency map generated by the disagreement of two classifiers to acquire few uncertain target pixel annotations.

Different from those prior works focusing on uncertain or diverse samples, our density-aware selection method acquires labels of few but vital samples that can bridge the gap between the source and target domains.

Active Learning for Domain Adaptation. Active learning can reduce the annotation effort by gradually selecting

the most valuable unlabeled data to be labeled.

Conventional active learning strategies can be roughly divided into two categories: uncertainty-based methods and diversity-aware approaches. The main idea of uncertainty-based methods is to acquire labels of data close to the model decision boundary. For example, [42, 44] utilized the softmax entropy, confidence, or margin of network outputs as the selection criterion. [13, 14] proposed a better measurement of uncertainty with MC-dropout. On the other hand, the key concept of diversity approaches is querying annotations of a batch of samples far away from each other in the feature space. Prior works used clustering [2] or greedy selection [19, 32, 46] to achieve the diversity in a query batch.

In addition, several recent works have studied active domain adaptation scenarios that consider both uncertainty and diversity. [38, 52] used the trained classifier and domain discriminator to select highly uncertain samples far from the source domain distribution. [12, 28, 37] utilized clustering to select highly uncertain samples that are diverse in target domain distribution. Recently, a concurrent work [47] proposed an energy-based approach with a conventional uncertainty measurement for this problem.

To the best of our knowledge, we propose the first density-aware active domain adaptation strategy to acquire labels of representative samples with high density in the target domain but low density in the source domain. Also, we developed the first adaptive budget allocation policy for active domain adaptation considering the adaptation difficulties across categories as well as the importance between density-aware and uncertainty-based methods.

3. Method

3.1. Overview

In this setting, we have a data pool of C -category semantic segmentation from two domains, comprising rich labeled data D_S in the source domain and some data D_T in the target domain. D_T can be divided into D_T^L and D_T^U , where D_T^L contains the data in the target domain that has been labeled and D_T^U stores the remaining unlabeled data.

Given the initial D_T without any annotations, *i.e.*, $D_T^L = \emptyset$, the ADA algorithm iteratively acquires annotations of few data in D_T^U to maximize the performance improvement over the test data in the target domain.

In this work, we treat a region in an image as the fundamental unit of label acquisition for data efficiency and label convenience following several prior works [3, 17, 22, 36]. As a preprocessing step, we divide an image into multiple regions using the widely-used SLIC [1] algorithm.

Our **Adaptive Density-aware Active Domain Adaptation (ADeADA)** framework can be divided into 4 steps: (1) Train an initial model on $D_S \cup D_T$ with UDA methods as a warmup step. (2) Perform the density-aware selection to

determine representative regions for each category according to the domain density. (Sec 3.2). (3) Determine the labeling budget for each category individually and adaptively weight the budget between density-aware and uncertainty-based methods. (Sec 3.3). (4) For the top-ranked regions in D_T^U , acquire ground truth labels and move them to D_T^L . Then, fine-tune the model on $D_S \cup D_T^L$ in a supervised manner and go back to step 2 for a new round (Sec 3.3.3).

3.2. Density-aware Selection

Our goal in the ADA problem is to adapt the model to the target domain with the least possible amount of queried annotations. In this work, we introduce a density-aware selection strategy to achieve this goal. The proposed strategy selects the most representative regions according to the estimated probability density in the source and target domains.

3.2.1 Domain Density Estimation

Domain density is a measurement of how common a region is predicted as a certain class in a particular domain. To derive the domain density, we first define the region feature z as the average feature over all the pixels within a region. Similarly, category $c \in \{1, 2, \dots, C\}$ is assigned to a region according to the predicted probability averaged across all of the pixels in the region.

Given a domain S , a feature vector z , and a category c , we define the **source domain density**

$$d_S = p_S(z|c) \quad (1)$$

as the probability that z is classified as c in S . To estimate $p_S(z|c)$, we construct the density estimators from all the observed (z, c) pairs in the source domain dataset. The target domain follows the manner similarly.

In our implementation, a set of Gaussian Mixture Models (GMMs) are served as the density estimators. The construction of GMMs can be efficiently completed by offline and parallel execution, which takes about 0.01 seconds per region with an 8-core CPU personal computer. More discussions and details are left in the supplemental material.

3.2.2 Density Difference as Metric

The core idea of our density-aware method is to select unlabeled target regions that are most efficient for domain adaptation. For the i -th unlabeled target region, we first obtained its source domain density d_S^i and d_T^i by feeding (z_i, c_i) to the pre-constructed density estimators.

Then, we rank the importance of all regions in D_T^U by an introduced metric:

$$\pi_i = \log\left(\frac{d_T^i}{d_S^i}\right). \quad (2)$$

Larger π indicates that a region is more prevalent in the target domain and less observable in the source domain. As a result, regions with large π can help us accomplish domain adaptation efficiently.

For each category c , unlabeled regions are sorted according to their importance scores. Then, the top-ranked regions for each category will be selected for labeling. We mathematically prove the effectiveness of our method in Sec 3.2.3.

3.2.3 Theoretical Foundation

To provide the theoretical foundations for our proposed density-aware selection, we leverage the proposition presented in [24]

$$\ell_{test} \leq \ell_{train} + \frac{M}{\sqrt{2}} \sqrt{D_{KL}(p_T(c, z) || p_S(c, z))}, \quad (3)$$

where ℓ_{test} and ℓ_{train} denote the testing and training loss respectively; p_S and p_T are the joint probability distributions of category c and feature z in the source and target domain, M is a constant term and $D_{KL}(||)$ is the KL divergence of the two distributions.

As shown in Eq 3, to provide a tighter generalization bound for ℓ_{test} , we aim to minimize the KL of the two joint probability distribution, which can be derived as:

$$D_{KL}(p_T(c, z) || p_S(c, z)) = D_{KL}(p_T(c) || p_S(c)) + \mathbb{E}_{p_T(c)}[D_{KL}(p_T(z|c) || p_S(z|c))]. \quad (4)$$

The proof is provided in the supplementary material.

Since $p_T(c)$ and $p_S(c)$ are similar in most cases, we can obtain better generalization to the target domain by minimizing the expected value of the KL divergence from $p_S(z|c)$ to $p_T(z|c)$. In the semantic segmentation task, in order to make the model perform well for each category and to deal with the label imbalance problem, we aim to reduce the KL term, *i.e.*, $D_{KL}(p_T(z|c) || p_S(z|c))$, for each category.

Although it is impossible to obtain the precise KL term by sampling all data points in the high dimensional continuous feature space, we could leverage the Monte Carlo simulation process to estimate the KL of the two distributions [16]. Given a sufficient number of N observed region features $\{z_i\}_{i=1}^N$ predicted to a certain category c , the KL divergence of the two conditional probability distributions can be approximated as

$$D_{KL}(p_T(z|c) || p_S(z|c)) \approx \frac{1}{N} \sum_{i=1}^N \log\left(\frac{p_T(z_i|c)}{p_S(z_i|c)}\right) = \frac{1}{N} \sum_{i=1}^N \pi_i, \quad (5)$$

where π is the metric to measure the importance of each region in our method mentioned in Sec 3.2.2.

Eq. 3, 4, 5 bridge the theory and our proposed method. By providing annotations for data that contribute the most to the KL divergence for each category, the domain shift between the source and target domain could be reduced, making the generalization bound of ℓ_{test} tighter.

3.3. Adaptive Budget Allocation

With our density-aware selection, the labeling budget in each round can be equally divided into C categories. Nonetheless, we demonstrate that ADA can be achieved more efficiently and economically by adaptively allocating budgets in each round. First, the data required for domain adaptation varies across categories, and thus it is inefficient to allocate the same budget to each class. Furthermore, a dynamic scheduling policy is developed to adjust the budget between density-aware and uncertainty-based selection on-the-fly. Therefore, we can benefit from the advantages of both selection strategies and avoid their weaknesses.

3.3.1 Category-balanced Selection

We empirically observe that the required budget for ADA could differ over categories. For example, the UDA methods can reach the performance close to fully supervised learning in some categories like vegetarian and building. However, it is difficult for them to generalize to some categories like train or sidewalk (see Table 1). Therefore, to fully utilize the labeling budget, we propose a category-balanced selection mechanism.

Intuitively, we would like to spend more budgets on hard categories, while fewer selection budgets for already well-aligned ones. According to Eq. 5, the average value of the region scores of a specific category can be regarded as an approximation of KL divergence from the source domain to the target domain. Therefore, we use this indicator to balance the selection budget across categories. Suppose the total labeling budget of our density selection in each round is B_d pixels, for a certain category c , the allocated budget $B_{d,c}$ is as follows:

$$B_{d,c} = \frac{\sigma(D_{KL}(p_T(z|c) || p_S(z|c)))}{\sum_{i=1}^C \sigma(D_{KL}(p_T(z|i) || p_S(z|i)))} \times B_d, \quad (6)$$

where σ is a normalization function to make the weighting term falls within a reasonable range.

The above equation ensures that the categories with larger domain shift are assigned to larger query budgets, while saving the budget for well-aligned categories.

3.3.2 Dynamic Scheduling Policy

Our dynamic scheduling policy decides the budgets for the conventional uncertainty measurement and our density-aware selection over time. The motivation is to take advantage of strengths of both and avoid their weaknesses.

As discussed before, reducing the domain gap is the main purpose of our density-aware method as illustrated in Figure 1 and the proof in Sec 3.2.3. Thus, the method achieves significant improvement in the early stages but performs worse in the later stages where the two domains are almost aligned as shown in rows 1 and 2 in Table 2. Conversely, as shown in Figure 2 (d, e, f), the strength of uncertainty is capturing the low-confident error with an accurate model in later stages, while the defect is the inability to detect high-confident error under severe domain shift, as shown in Figure 2 (a, b, c).

Based on the analysis, we design a dynamic scheduling policy to integrate the density-aware and uncertainty-based methods. Let B^k be the labeling budget of the k -th active selection round, including B_d^k for the density-aware approach and B_u^k for an uncertainty-based method. We arrange the budget allocation for the two methods as follows:

$$B_d^k = \alpha \cdot 2^{-\beta(k-1)} \cdot B^k, \quad B_u^k = B^k - B_d^k, \quad (7)$$

where α is the balance coefficient between density-aware and the uncertainty-based method, and β is the decay rate of the labeling budget of the density-aware approach. The reason for using half decay is to reflect the observation of the rapid domain shift reduction, which is discussed in Sec 4.4. The above formula ensures that the density-aware method is relied on when the domain gaps are large in the early stage, and the uncertainty-based method is mainly used when the gaps are diminished in the later stage. This technique further boosted the label efficiency under fixed annotation budgets. In our implementation, we use the conventional softmax entropy [42] as the uncertainty measurement.

3.3.3 Label Acquisition

After completing the density-aware selection and the adaptive budget allocation policy, we acquire the ground truth labels of the top-ranked regions until the budget B is exhausted. Then, we move these annotated regions from the unlabeled target set D_T^U to the labeled target set D_T^L . Finally, we fine-tune the model with $D_S \cup D_T^L$ under supervision and then execute the next active selection round.

4. Experiments

4.1. Experimental Settings

We elaborate the datasets, networks and active learning protocol in our experiments. The implementation details are reported in the supplementary material due to limited space.

Datasets. We evaluated various active learning and domain adaptation methods on two widely-used domain adaptive semantic segmentation benchmarks: GTA5 \rightarrow Cityscapes and SYNTHIA \rightarrow Cityscapes. Cityscapes [10] is a real-world self-driving dataset containing 2975 labeled training images, 500 labeled validation images and 1225 test images. GTA5 [29] is a synthetic dataset consisting of 24966 annotated images, which shares 19 semantic categories with Cityscapes. SYNTHIA dataset [30] has 9400 synthetic annotated images, which shares 16 semantic categories with Cityscapes. For a fair comparison, we evaluated all methods on the Cityscapes validation split.

Network Backbones. We evaluated all active learning strategies with DeepLabV3+ [8], a semantic segmentation model. To fairly compare our method with existing domain adaptation approaches, we report the results of our method on both DeepLabV2 [6] and DeepLabV3+ [8]. The two models are based on the ResNet-101 [15] backbone.

Active Learning Protocol. For all experiments, we first adopted [40] to train the network with adversarial training as a warmup step. Then we performed K -round active selection comprised of the following steps: (1) Select a small portion x_{active} of the data from D_T^U based on different active selection strategies. (2) Acquire the labels of these selected data and add them to D_T^L . (3) Fine-tune the model with $D_S \cup D_T^L$ in a supervised manner. In our setting, we chose $K = 5$, $x_{active} = 1\%$ for both the two tasks.

4.2. Comparison with Active Learning Baselines

We compared ADeADA with 8 other active learning strategies, including random region selection (RAND), uncertainty-based methods (CONF [42], MAR [42], and ENT [42]), hybrid methods (BADGE [2] and ReDAL [46]), and existing Active Domain Adaptation baselines (AADA [38] and CLUE [28]). The implementation details are described in the supplementary material.

The experimental results are shown in Figure 3. In each subplot, the x-axis indicates the percentage of total target domain annotated points and the y-axis is the corresponding mIoU score achieved by the network.

The improvement of our proposed ADeADA is significant compared to prior active learning strategies. Under 5% labels, ADeADA surpassed the second-placed approach by 0.55 mIoU in GTA \rightarrow Cityscapes, whereas the gap between the second and fourth place was only 0.2. Similarly, in SYNTHIA \rightarrow Cityscapes, ADeADA outperformed second place by 0.98 mIoU, while the difference between the second and fourth place was 0.39. Moreover, our method consistently prevailed over other methods by more than 0.5 mIoU under all experiments. The results verify our method makes huge progress in active domain adaptation problems.

On the GTA5 \rightarrow Cityscapes, our proposed ADeADA surpasses uncertainty-based active learning methods (ENT,

CONF, and MAR) for over 3% mIoU at the first round. This suggests that density as a selection metric clearly benefits ADA over uncertainty against domain shift in early stages.

Compared with existing ADA methods (AADA, CLUE) or hybrid active learning approaches (ReDAL, BADGE), our method also achieves better performance under any tasks and with any amount of budget. On the two tasks, AADA even performs worse than random selection in the early stage. We conjecture that the selected biased samples might be inconsistent with the real target distribution as shown in Figure 1 (a). As for the other methods (CLUE, ReDAL, BADGE), because they only considered selecting diverse target domain data but did not avoid selecting samples that were likely to appear in the source distribution shown as Figure 1 (b). These strategies might cause redundant annotations on well-learned samples and made the performance inferior to ours.

4.3. Comparison with Domain Adaptation Methods

We also compared our developed ADeADA with existing domain adaptation methods, including unsupervised domain adaptations (UDAs) [18, 23, 35, 40, 41, 48, 50, 54], weakly-supervised domain adaptation (WDA) [26], semi-supervised domain adaptation (SSDA) [9, 45] and active domain adaptations (ADA) [25, 34, 47]¹.

The results of GTA5 \rightarrow Cityscapes can be shown in Table 1 (a). Compared with the current state-of-the-art UDA method [50], our method achieves an advantage of more than 10% mIoU with only 5% annotation effort. Furthermore, the performance of our method can achieve over 97% of the result of full supervision on target labeled data on both DeepLabV2 and DeepLabV3+ models. Compared with other label-efficient approaches (WDA, SSDA, ADA), our method not only performs better on overall mIoU score but also has obvious improvement on small objects, such as “rider” or “bicycle”, and difficult categories, like “fence”, “sidewalks” and “train”, as visualized in Figure 4.

The results of SYNTHIA \rightarrow Cityscapes is shown in Table 1 (b). Our method also outperforms any existing UDA methods over 10% mIoU score and achieves over 97% of the result of full supervision on target labeled data with merely 5% annotations. Also, compared with other label-efficient approaches (WDA, SSDA, ADA), our method performs better on the overall mIoU score, especially on difficult categories or small objects like “bus” and “pole”.

In addition, since the protocols used in prior label-efficient methods differ, Figure 5 makes a fair comparison of these methods. The x-axis indicates the percentage of total target domain annotated points and the y-axis is the corresponding mIoU score achieved by the network. Obviously, our approach achieves higher performance over exist-

¹We report the official results of the UDA, WDA, SSDA and ADA methods and train the DeepLabV2 and DeepLabV3+ ourselves.

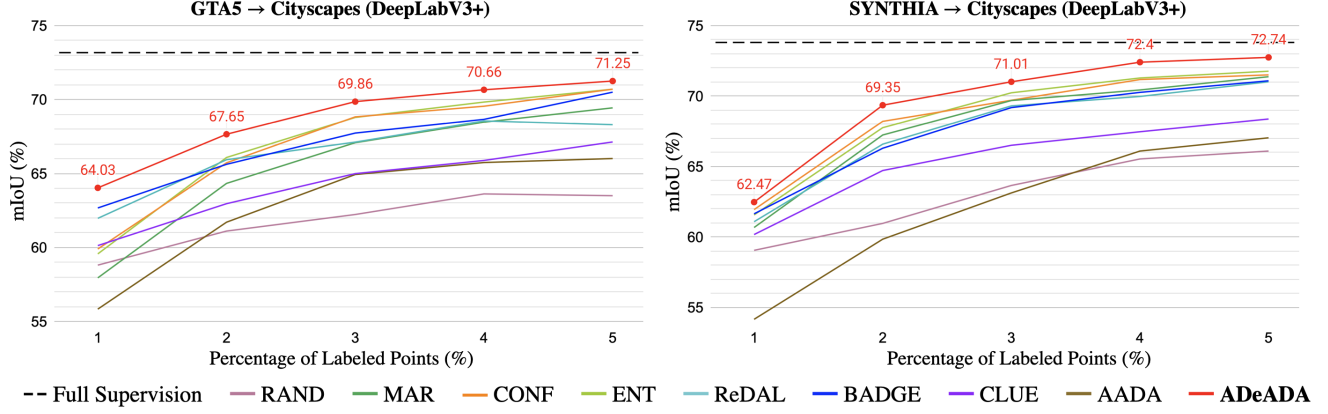


Figure 3. **Comparison with different active learning baselines.** Experimental results show that under the same region-level active learning protocol, our proposed ADeADA outperforms 8 existing active learning strategies on two widely-used benchmarks. Due to space limitations, we left the complete experimental results in the supplementary material.

(a) GTA5 → Cityscapes																					
	Method	Road	SW	Build	Wall	Fence	Pole	TL	TS	Veg.	Terrain	Sky	PR	Rider	Car	Truck	Bus	Train	Motor	Bike	mIoU
UDA	AdaptSeg [40]	86.5	36.0	79.9	23.4	23.3	35.2	14.8	14.8	83.4	33.3	75.6	58.5	27.6	73.7	32.5	35.4	3.9	30.1	28.1	42.4
	ADVENT [41]	89.9	36.5	81.2	29.2	25.2	28.5	32.3	22.4	83.9	34.0	77.1	57.4	27.9	83.7	29.4	39.1	1.5	28.4	23.3	43.8
	CRST [54]	91.0	55.4	80.0	33.7	21.4	37.3	32.9	24.5	85.0	34.1	80.8	57.7	24.6	84.1	27.8	30.1	26.9	26.0	42.3	47.1
	LTIR [18]	92.9	55.0	85.3	34.2	31.1	34.9	40.7	34.0	85.2	40.1	87.1	61.0	31.1	82.5	32.3	42.9	0.3	36.4	46.1	50.2
	FDA [48]	92.5	53.3	82.4	26.5	27.6	36.4	40.6	38.9	82.3	39.8	78.0	62.6	34.4	84.9	34.1	53.1	16.9	27.7	46.4	50.5
	TPLD [35]	94.2	60.5	82.8	36.6	16.6	39.3	29.0	25.5	85.6	44.9	84.4	60.6	27.4	84.1	37.0	47.0	31.2	36.1	50.3	51.2
	IAST [23]	93.8	57.8	85.1	39.5	26.7	26.2	43.1	34.7	84.9	32.9	88.0	62.6	29.0	87.3	39.2	49.6	23.2	34.7	39.6	51.5
	ProDA [50]	87.8	56.0	79.7	46.3	44.8	45.6	53.5	53.5	88.6	45.2	82.1	70.7	39.2	88.8	45.5	59.4	1.0	48.9	56.4	57.5
WDA	WDA [26] (Point)	94.0	62.7	86.3	36.5	32.8	38.4	44.9	51.0	86.1	43.4	87.7	66.4	36.5	87.9	44.1	58.8	23.2	35.6	55.9	56.4
SSDA	ASS [45] (+50 city)	94.3	63.0	84.5	26.8	28.0	38.4	35.5	48.7	87.1	39.2	88.8	62.2	16.3	87.6	23.2	39.2	7.2	24.4	58.1	50.1
ADA	LabOR [34] (V2, 2.2%)	96.6	77.0	89.6	47.8	50.7	48.0	56.6	63.5	89.5	57.8	91.6	72.0	47.3	91.7	62.1	61.9	48.9	47.9	65.3	66.6
	MADA [25] (V3+, 5%)	95.1	69.8	88.5	43.3	48.7	45.7	53.3	59.2	89.1	46.7	91.5	73.9	50.1	91.2	60.6	56.9	48.4	51.6	68.7	64.9
	ADeADA (V2, 5%)	96.3	73.6	89.3	50.0	52.3	48.0	56.9	64.7	89.3	53.9	92.3	73.9	52.9	91.8	69.7	78.9	62.7	57.7	71.1	69.7
	ADeADA (V3+, 5%)	97.0	77.8	90.0	46.0	55.0	52.7	58.7	65.8	90.4	58.9	92.1	75.7	54.4	92.3	69.0	78.0	68.5	59.1	72.3	71.3
Target Only	DeepLabV2 [6]	97.4	79.5	90.3	51.1	52.4	49.0	57.5	68.0	90.5	58.1	93.1	75.1	53.9	92.7	72.0	80.2	65.0	58.1	71.1	71.3
	DeepLabV3+ [8]	97.6	81.3	91.1	49.8	57.6	53.8	59.6	69.1	91.2	60.5	94.4	76.7	55.6	93.3	75.8	79.9	72.9	57.7	72.2	73.2

(b) SYNTHIA → Cityscapes																					
	Method	Road	SW	Build	Wall*	Fence*	Pole*	TL	TS	Veg.	Sky	PR	Rider	Car	Bus	Motor	Bike	mIoU	mIoU*		
UDA	AdaptSeg [40]	79.2	37.2	78.8	-	-	-	9.9	10.5	78.2	80.5	53.5	19.6	67.0	29.5	21.6	31.3	-	45.9		
	ADVENT [41]	85.6	42.2	79.7	8.7	0.4	25.9	5.4	8.1	80.4	84.1	57.9	23.8	73.3	36.4	14.2	33.0	41.2	48.0		
	CRST [54]	67.7	32.2	73.9	10.7	1.6	37.4	22.2	31.2	80.8	80.5	60.8	29.1	82.8	25.0	19.4	45.3	43.8	50.1		
	LTIR [18]	92.6	53.2	79.2	-	-	-	1.6	7.5	78.6	84.4	52.6	20.0	82.1	34.8	14.6	39.4	-	49.3		
	FDA [48]	79.3	35.0	73.2	-	-	-	19.9	24.0	61.7	82.6	61.4	31.1	83.9	40.8	38.4	51.1	-	52.5		
	TPLD [35]	80.9	44.3	82.2	19.9	0.3	40.6	20.5	30.1	77.2	80.9	60.6	25.5	84.8	41.1	24.7	43.7	47.3	53.5		
	IAST [23]	81.9	41.5	83.3	17.7	4.6	32.3	30.9	28.8	83.4	85.0	65.5	30.8	86.5	38.2	33.1	52.7	49.8	57.0		
	ProDA [50]	87.8	45.7	84.6	37.1	0.6	44.0	54.6	37.0	88.1	84.4	74.2	24.3	88.2	51.1	40.5	45.6	55.5	62.0		
WDA	WDA [26] (Point)	94.9	63.2	85.0	27.3	24.2	34.9	37.3	50.8	84.4	88.2	60.6	36.3	86.4	43.2	36.5	61.3	57.2	63.7		
SSDA	ASS [45] (+50 city)	94.1	63.9	87.6	-	-	-	18.1	37.1	87.5	89.7	64.6	37.0	87.4	38.6	23.2	59.6	-	60.7		
ADA	MADA [25] (V3+, 5%)	96.5	74.6	88.8	45.9	43.8	46.7	52.4	60.5	89.7	92.2	74.1	51.2	90.9	60.3	52.4	69.4	68.1	73.3		
	ADeADA (V2, 5%)	96.4	76.3	89.1	42.5	47.7	48.0	55.6	66.5	89.5	91.7	75.1	55.2	91.4	77.0	58.0	71.8	70.6	76.3		
	ADeADA (V3+, 5%)	96.7	76.8	90.3	48.7	51.1	54.2	58.3	68.0	90.4	93.4	77.4	56.4	92.5	77.5	58.9	73.3	72.7	77.7		
Target Only	DeepLabV2 [6]	97.4	79.5	90.3	51.1	52.4	49.0	57.5	68.0	90.5	93.1	75.1	53.9	92.7	80.2	58.1	71.1	72.5	77.5		
	DeepLabV3+ [8]	97.6	81.3	91.1	49.8	57.6	53.8	59.6	69.1	91.2	94.4	76.7	55.6	93.3	79.9	57.7	72.2	73.8	78.4		

Table 1. **Comparison with different domain adaptation approaches on (a) GTA5 → Cityscapes and (b) SYNTHIA → Cityscapes.** Our proposed ADeADA outperforms any existing methods on the overall mIoU and most per-class IoU with only 5% target annotations with different network backbones. mIoU* in (b) denotes the averaged scores across 13 categories used in [40]. To fairly compare all methods under the same number of annotations, we draw a chart in Figure 5.

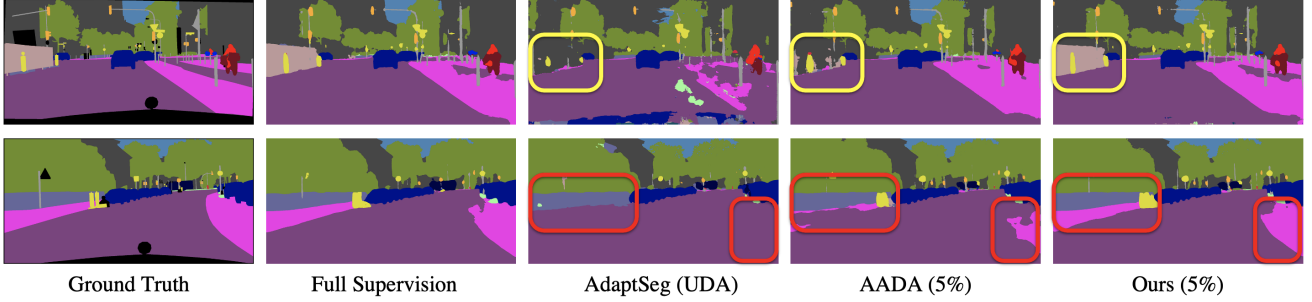


Figure 4. **Qualitative results of different approaches for the GTA5 → Cityscapes domain adaptation task.** Compared with the UDA method [40] and the previous ADA approach [38], our learning method makes the model recognize hard categories, such as “fence” (shown on the yellow bounding box in the first row) and almost perfectly distinguish “sidewalks” from “roads” (shown on the red bounding box in the second row) with only 5% labeled points.

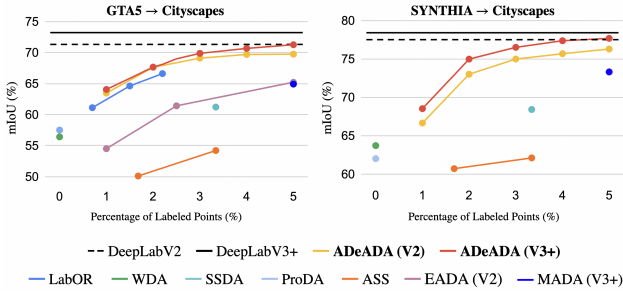


Figure 5. **Comparison with different label-efficient methods.** We compare our method with the state-of-the-art UDA method, ProDA [50] as well as various label-efficient approaches, including WDA [26], SSDA [9], ASS [45], MADA [25], LabOR [34] and EADA [47]. On two tasks and networks, our proposed ADeADA achieves the best result under the same number of labels.

	Components				mIoU		
	uncertainty	density aware	category balance	dynamic scheduling	1%	3%	5%
(a)	✓				59.97	68.79	70.70
(b)		✓			62.75	68.81	69.82
(c)		✓	✓		64.03	69.38	70.69
(d)	✓	✓	✓		63.30	69.66	71.15
(e)	✓	✓	✓	✓	64.03	69.86	71.25

Table 2. **Ablation studies.** The three columns on the right show the model performance when 1%, 3%, and 5% target annotations are acquired by different active selection strategies. The results validate the effectiveness of our density-aware method and adaptive budget allocation policy as the discussion in Sec 4.4.

ing methods with the same number of labeled pixels. Also, each region contains only 3.1 different categories on average, and about 50% regions are with less than two categories. Thus, with the same number of labeled pixels, our region-level approach requires much less effort than pixel-level approaches, such as LabOR [34].

4.4. Ablation Studies

We also conducted ablation studies to validate the effectiveness of our proposed components with DeepLabV3+ backbone on GTA5 → Cityscapes as shown in Table 2.

From the comparison of (a) and (b), the pure density-aware method prevailed the pure uncertainty-based one by 2.78 mIoU in the first stage, while slightly worse than uncertainty in the final stage. The result demonstrated the effectiveness of our density-aware selection and echoed our intuition of combining the two methods.

As can be observed from (b) and (c), our category-balanced selection strategy boosted the model performance by over 0.5 mIoU in any situation. The result suggested that spending more labeling budgets on hard categories but few budgets for already well-aligned ones is indeed effective.

As discussed in Sec 3.3, we designed an dynamic scheduling policy to take the advantage of both uncertainty and density. As shown in (c) and (e), combining the two methods with our designed policy achieved the best result under any situations. Additionally, the comparison of (d) and (e) validates our policy surpassed the “equally distributed” budget allocation baseline. Extensive experiments and discussions about hyper-parameter settings and budget allocation strategies are left in the supplementary material.

Overall, the ablation studies suggested that the proposed density-aware technique and traditional uncertainty-based method complement each other to reach better adaptability under our budget allocation policy.

5. Conclusion

We propose ADeADA, a novel active domain adaptation method for semantic segmentation. By labeling samples with high probability density in the target domain yet with low probability density in the source domain, models can conquer the domain shift with limited annotation effort. Furthermore, we design the first adaptive budget allocation policy to balance labeling budgets among different categories and between different active learning methods.

Acknowledgement

This work was supported in part by the Ministry of Science and Technology, Taiwan, under Grant MOST 110-2634-F-002-051, Mobile Drive Technology, and Industrial Technology Research Institute (ITRI). We are grateful to the National Center for High-performance Computing.

References

- [1] Radhakrishna Achanta, Appu Shaji, Kevin Smith, Aurelien Lucchi, Pascal Fua, and Sabine Süsstrunk. Slic superpixels compared to state-of-the-art superpixel methods. *IEEE transactions on pattern analysis and machine intelligence*, 34(11):2274–2282, 2012. 3
- [2] Jordan T Ash, Chicheng Zhang, Akshay Krishnamurthy, John Langford, and Alekh Agarwal. Deep batch active learning by diverse, uncertain gradient lower bounds. In *ICLR*, 2020. 2, 3, 6, 14
- [3] Arantxa Casanova, Pedro O. Pinheiro, Negar Rostamzadeh, and Christopher J. Pal. Reinforced active learning for image segmentation. In *International Conference on Learning Representations*, 2020. 3
- [4] Wei-Lun Chang, Hui-Po Wang, Wen-Hsiao Peng, and Wei-Chen Chiu. All about structure: Adapting structural information across domains for boosting semantic segmentation. In *Proceedings of the IEEE/CVF Conference on Computer Vision and Pattern Recognition*, pages 1900–1909, 2019. 1, 3
- [5] Liang-Chieh Chen, George Papandreou, Iasonas Kokkinos, Kevin Murphy, and Alan L Yuille. Deeplab: Semantic image segmentation with deep convolutional nets, atrous convolution, and fully connected crfs. *IEEE transactions on pattern analysis and machine intelligence*, 40(4):834–848, 2017. 1
- [6] Liang-Chieh Chen, George Papandreou, Iasonas Kokkinos, Kevin P. Murphy, and Alan Loddon Yuille. Semantic image segmentation with deep convolutional nets and fully connected crfs. *CoRR*, abs/1412.7062, 2015. 1, 6, 7
- [7] Liang-Chieh Chen, George Papandreou, Florian Schroff, and Hartwig Adam. Rethinking atrous convolution for semantic image segmentation. *arXiv preprint arXiv:1706.05587*, 2017. 1
- [8] Liang-Chieh Chen, Yukun Zhu, George Papandreou, Florian Schroff, and Hartwig Adam. Encoder-decoder with atrous separable convolution for semantic image segmentation. In *Proceedings of the European conference on computer vision (ECCV)*, pages 801–818, 2018. 1, 6, 7
- [9] Shuaijun Chen, Xu Jia, Jianzhong He, Yongjie Shi, and Jianzhuang Liu. Semi-supervised domain adaptation based on dual-level domain mixing for semantic segmentation. In *Proceedings of the IEEE/CVF Conference on Computer Vision and Pattern Recognition*, pages 11018–11027, 2021. 3, 6, 8
- [10] Marius Cordts, Mohamed Omran, Sebastian Ramos, Timo Rehfeld, Markus Enzweiler, Rodrigo Benenson, Uwe Franke, Stefan Roth, and Bernt Schiele. The cityscapes dataset for semantic urban scene understanding. In *Proceedings of the IEEE conference on computer vision and pattern recognition*, pages 3213–3223, 2016. 1, 6, 18
- [11] Liang Du, Jingang Tan, Hongye Yang, Jianfeng Feng, Xiangyang Xue, Qibao Zheng, Xiaoqing Ye, and Xiaolin Zhang. Ssf-dan: Separated semantic feature based domain adaptation network for semantic segmentation. In *Proceedings of the IEEE/CVF International Conference on Computer Vision*, pages 982–991, 2019. 1, 3
- [12] Bo Fu, Zhangjie Cao, Jianmin Wang, and Mingsheng Long. Transferable query selection for active domain adaptation. In *Proceedings of the IEEE/CVF Conference on Computer Vision and Pattern Recognition*, pages 7272–7281, 2021. 1, 2, 3
- [13] Yarin Gal and Zoubin Ghahramani. Dropout as a bayesian approximation: Representing model uncertainty in deep learning. In *international conference on machine learning*, pages 1050–1059, 2016. 2, 3
- [14] Yarin Gal, Riashat Islam, and Zoubin Ghahramani. Deep bayesian active learning with image data. In *International Conference on Machine Learning*, pages 1183–1192, 2017. 3
- [15] Kaiming He, Xiangyu Zhang, Shaoqing Ren, and Jian Sun. Deep residual learning for image recognition. In *Proceedings of the IEEE conference on computer vision and pattern recognition*, pages 770–778, 2016. 6
- [16] John R Hershey and Peder A Olsen. Approximating the kullback leibler divergence between gaussian mixture models. In *2007 IEEE International Conference on Acoustics, Speech and Signal Processing-ICASSP'07*, volume 4, pages IV–317. IEEE, 2007. 4
- [17] Tejaswi Kasarla, Gattigorla Nagendar, Guruprasad M Hegde, Vineeth Balasubramanian, and CV Jawahar. Region-based active learning for efficient labeling in semantic segmentation. In *2019 IEEE Winter Conference on Applications of Computer Vision (WACV)*, pages 1109–1117. IEEE, 2019. 3
- [18] Myeongjin Kim and Hyeran Byun. Learning texture invariant representation for domain adaptation of semantic segmentation. In *Proceedings of the IEEE/CVF Conference on Computer Vision and Pattern Recognition*, pages 12975–12984, 2020. 1, 6, 7
- [19] Andreas Kirsch, Joost van Amersfoort, and Yarin Gal. Batchbald: Efficient and diverse batch acquisition for deep bayesian active learning. In *Advances in Neural Information Processing Systems*, pages 7026–7037, 2019. 2, 3
- [20] Guosheng Lin, Anton Milan, Chunhua Shen, and Ian Reid. Refinenet: Multi-path refinement networks for high-resolution semantic segmentation. In *Proceedings of the IEEE conference on computer vision and pattern recognition*, pages 1925–1934, 2017. 1
- [21] Yawei Luo, Liang Zheng, Tao Guan, Junqing Yu, and Yi Yang. Taking a closer look at domain shift: Category-level adversaries for semantics consistent domain adaptation. In *Proceedings of the IEEE/CVF Conference on Computer Vision and Pattern Recognition*, pages 2507–2516, 2019. 1, 3
- [22] Radek Mackowiak, Philip Lenz, Omair Ghori, Ferran Diego, Oliver Lange, and Carsten Rother. CEREALS - cost-

- effective region-based active learning for semantic segmentation. In *British Machine Vision Conference 2018, BMVC 2018, Newcastle, UK, September 3-6, 2018*, page 121. BMVA Press, 2018. [3](#)
- [23] Ke Mei, Chuang Zhu, Jiaqi Zou, and Shanghang Zhang. Instance adaptive self-training for unsupervised domain adaptation. In *Computer Vision–ECCV 2020: 16th European Conference, Glasgow, UK, August 23–28, 2020, Proceedings, Part XXVI 16*, pages 415–430. Springer, 2020. [1](#), [6](#), [7](#)
- [24] A Tuan Nguyen, Toan Tran, Yarin Gal, Philip HS Torr, and Atılım Güneş Baydin. Kl guided domain adaptation. *arXiv preprint arXiv:2106.07780*, 2021. [4](#)
- [25] Munan Ning, Donghuan Lu, Dong Wei, Cheng Bian, Chenglang Yuan, Shuang Yu, Kai Ma, and Yefeng Zheng. Multi-anchor active domain adaptation for semantic segmentation. In *Proceedings of the IEEE/CVF International Conference on Computer Vision*, pages 9112–9122, 2021. [2](#), [3](#), [6](#), [7](#), [8](#)
- [26] Sujoy Paul, Yi-Hsuan Tsai, Samuel Schuster, Amit K Roy-Chowdhury, and Manmohan Chandraker. Domain adaptive semantic segmentation using weak labels. In *Computer Vision–ECCV 2020: 16th European Conference, Glasgow, UK, August 23–28, 2020, Proceedings, Part IX 16*, pages 571–587. Springer, 2020. [3](#), [6](#), [7](#), [8](#)
- [27] Fabian Pedregosa, Gaël Varoquaux, Alexandre Gramfort, Vincent Michel, Bertrand Thirion, Olivier Grisel, Mathieu Blondel, Peter Prettenhofer, Ron Weiss, Vincent Dubourg, et al. Scikit-learn: Machine learning in python. *Journal of machine learning research*, 12(Oct):2825–2830, 2011. [12](#)
- [28] Viraj Prabhu, Arjun Chandrasekaran, Kate Saenko, and Judy Hoffman. Active domain adaptation via clustering uncertainty-weighted embeddings. In *Proceedings of the IEEE/CVF International Conference on Computer Vision*, pages 8505–8514, 2021. [1](#), [2](#), [3](#), [6](#), [14](#)
- [29] Stephan R Richter, Vibhav Vineet, Stefan Roth, and Vladlen Koltun. Playing for data: Ground truth from computer games. In *European conference on computer vision*, pages 102–118. Springer, 2016. [1](#), [6](#), [18](#)
- [30] German Ros, Laura Sellart, Joanna Materzynska, David Vazquez, and Antonio M Lopez. The synthia dataset: A large collection of synthetic images for semantic segmentation of urban scenes. In *Proceedings of the IEEE conference on computer vision and pattern recognition*, pages 3234–3243, 2016. [6](#), [18](#)
- [31] Dan Roth and Kevin Small. Margin-based active learning for structured output spaces. In *European Conference on Machine Learning*, pages 413–424. Springer, 2006. [2](#)
- [32] Ozan Sener and Silvio Savarese. Active learning for convolutional neural networks: A core-set approach. In *International Conference on Learning Representations*, 2018. [2](#), [3](#)
- [33] Claude E Shannon. A mathematical theory of communication. *The Bell system technical journal*, 27(3):379–423, 1948. [14](#)
- [34] Inkyu Shin, Dong-Jin Kim, Jae Won Cho, Sanghyun Woo, Kwanyong Park, and In So Kweon. Labor: Labeling only if required for domain adaptive semantic segmentation. In *Proceedings of the IEEE/CVF International Conference on Computer Vision*, pages 8588–8598, 2021. [2](#), [3](#), [6](#), [7](#), [8](#)
- [35] Inkyu Shin, Sanghyun Woo, Fei Pan, and In So Kweon. Two-phase pseudo label densification for self-training based domain adaptation. In *European conference on computer vision*, pages 532–548. Springer, 2020. [1](#), [6](#), [7](#)
- [36] Yawar Siddiqui, Julien Valentin, and Matthias Nießner. Viewal: Active learning with viewpoint entropy for semantic segmentation. In *Proceedings of the IEEE/CVF Conference on Computer Vision and Pattern Recognition*, pages 9433–9443, 2020. [2](#), [3](#)
- [37] Anurag Singh, Naren Doraiswamy, Sawa Takamuku, Megh Bhalerao, Titir Dutta, Soma Biswas, Aditya Chepuri, Balasubramanian Vengatesan, and Naotake Natori. Improving semi-supervised domain adaptation using effective target selection and semantics. In *Proceedings of the IEEE/CVF Conference on Computer Vision and Pattern Recognition*, pages 2709–2718, 2021. [1](#), [2](#), [3](#)
- [38] Jong-Chyi Su, Yi-Hsuan Tsai, Kihyuk Sohn, Buyu Liu, Subhansu Maji, and Manmohan Chandraker. Active adversarial domain adaptation. In *Proceedings of the IEEE/CVF Winter Conference on Applications of Computer Vision*, pages 739–748, 2020. [1](#), [2](#), [3](#), [6](#), [8](#), [14](#), [15](#)
- [39] Ke Sun, Bin Xiao, Dong Liu, and Jingdong Wang. Deep high-resolution representation learning for human pose estimation. In *Proceedings of the IEEE/CVF Conference on Computer Vision and Pattern Recognition*, pages 5693–5703, 2019. [1](#)
- [40] Yi-Hsuan Tsai, Wei-Chih Hung, Samuel Schuster, Kihyuk Sohn, Ming-Hsuan Yang, and Manmohan Chandraker. Learning to adapt structured output space for semantic segmentation. In *Proceedings of the IEEE conference on computer vision and pattern recognition*, pages 7472–7481, 2018. [1](#), [3](#), [6](#), [7](#), [8](#), [12](#), [13](#), [15](#), [16](#)
- [41] Tuan-Hung Vu, Himalaya Jain, Maxime Bucher, Matthieu Cord, and Patrick Pérez. Advent: Adversarial entropy minimization for domain adaptation in semantic segmentation. In *Proceedings of the IEEE/CVF Conference on Computer Vision and Pattern Recognition*, pages 2517–2526, 2019. [1](#), [3](#), [6](#), [7](#)
- [42] D. Wang and Y. Shang. A new active labeling method for deep learning. In *2014 International Joint Conference on Neural Networks (IJCNN)*, pages 112–119, 2014. [2](#), [3](#), [5](#), [6](#), [13](#), [14](#)
- [43] Jingdong Wang, Ke Sun, Tianheng Cheng, Borui Jiang, Chaorui Deng, Yang Zhao, Dong Liu, Yadong Mu, Mingkui Tan, Xinggang Wang, et al. Deep high-resolution representation learning for visual recognition. *IEEE transactions on pattern analysis and machine intelligence*, 2020. [1](#)
- [44] Keze Wang, Dongyu Zhang, Ya Li, Ruimao Zhang, and Liang Lin. Cost-effective active learning for deep image classification. *IEEE Transactions on Circuits and Systems for Video Technology*, 27(12):2591–2600, 2016. [2](#), [3](#), [14](#)
- [45] Zhonghao Wang, Yunchao Wei, Rogerio Feris, Jinjun Xiong, Wen-Mei Hwu, Thomas S Huang, and Honghui Shi. Alleviating semantic-level shift: A semi-supervised domain adaptation method for semantic segmentation. In *Proceedings of the IEEE/CVF International Conference on Computer Vision*, pages 8588–8598, 2021. [2](#), [3](#), [6](#), [7](#), [8](#)

- the *IEEE/CVF Conference on Computer Vision and Pattern Recognition Workshops*, pages 936–937, 2020. 3, 6, 7, 8
- [46] Tsung-Han Wu, Yueh-Cheng Liu, Yu-Kai Huang, Hsin-Ying Lee, Hung-Ting Su, Ping-Chia Huang, and Winston H Hsu. Redal: Region-based and diversity-aware active learning for point cloud semantic segmentation. In *Proceedings of the IEEE/CVF International Conference on Computer Vision*, pages 15510–15519, 2021. 2, 3, 6, 14
- [47] Binhui Xie, Longhui Yuan, Shuang Li, Chi Harold Liu, Xin-jing Cheng, and Guoren Wang. Active learning for domain adaptation: An energy-based approach. *arXiv preprint arXiv:2112.01406*, 2021. 3, 6, 8
- [48] Yanchao Yang and Stefano Soatto. Fda: Fourier domain adaptation for semantic segmentation. In *Proceedings of the IEEE/CVF Conference on Computer Vision and Pattern Recognition*, pages 4085–4095, 2020. 1, 6, 7
- [49] Yuhui Yuan, Xiaokang Chen, Xilin Chen, and Jingdong Wang. Segmentation transformer: Object-contextual representations for semantic segmentation. In *European Conference on Computer Vision (ECCV)*, volume 1, 2021. 1
- [50] Pan Zhang, Bo Zhang, Ting Zhang, Dong Chen, Yong Wang, and Fang Wen. Prototypical pseudo label denoising and target structure learning for domain adaptive semantic segmentation. In *Proceedings of the IEEE/CVF Conference on Computer Vision and Pattern Recognition*, pages 12414–12424, 2021. 1, 3, 6, 7, 8
- [51] Hengshuang Zhao, Jianping Shi, Xiaojuan Qi, Xiaogang Wang, and Jiaya Jia. Pyramid scene parsing network. In *Proceedings of the IEEE conference on computer vision and pattern recognition*, pages 2881–2890, 2017. 1
- [52] Fan Zhou, Changjian Shui, Shichun Yang, Bincheng Huang, Boyu Wang, and Brahim Chaib-draa. Discriminative active learning for domain adaptation. *Knowledge-Based Systems*, 222:106986, 2021. 1, 2, 3
- [53] Yang Zou, Zhiding Yu, BVK Kumar, and Jinsong Wang. Unsupervised domain adaptation for semantic segmentation via class-balanced self-training. In *Proceedings of the European conference on computer vision (ECCV)*, pages 289–305, 2018. 1, 3
- [54] Yang Zou, Zhiding Yu, Xiaofeng Liu, BVK Kumar, and Jinsong Wang. Confidence regularized self-training. In *Proceedings of the IEEE/CVF International Conference on Computer Vision*, pages 5982–5991, 2019. 1, 3, 6, 7

Supplementary Material

A. Implementation Details

We conducted all experiments on an 8-core CPU personal computer with an NVIDIA RTX3090 GPU. The following section elaborates on the implementation details of UDA warm-up, density-aware selection, adaptive budget decision and network fine-tuning. Note that the following symbols are identical to those in Section 3 of the main paper. The whole pipeline is presented in Algorithm 1.

UDA warm-up For the two tasks, GTA5 \rightarrow Cityscapes and SYNTHIA \rightarrow Cityscapes, we utilized a conventional UDA method [40] to train an initial model. For both DeepLabV2 and DeepLabV3+ network backbones, we apply the SGD optimizer with the initial learning rate as $2.5e-4$ and the decay rate 0.9. Following [40], we use cross-entropy loss and adversarial loss as loss functions and warm up the network with adversarial training for about 100k steps.

Density-aware selection As mentioned in Section 3.1 of the main paper, we utilized a set of Gaussian Mixture Models (GMMs) to model the domain density $p_S(z|c)$ and $p_T(z|c)$ separately. The categorical domain density measures how common a region is predicted as a certain class in a particular domain.

The region feature z is a vector of 256 dimensions. For the DeepLabV3+ network backbone, the feature is extracted before the final linear classification layer. For the DeepLabV2 network backbone, we slightly modify the network to make the output of Atrous Spatial Pyramid Pooling (ASPP) as a 256-dimensional feature vector and add the final classification layer after ASPP.

We use a widely-used python package, scikit-learn [27], to construct a set of GMMs. In our implementation, the number of mixtures, which is a pre-defined hyper-parameter of the GMM, is proportional to the number of regions of the category and is clipped in the range of 1 to 10. The process of constructing GMMs can be efficiently completed by offline and parallel execution, which takes about 0.01 seconds per region with four parallel processes. We believe that the density estimator could be replaced by other methods and is worth further investigation, which is beyond the scope of this paper.

Adaptive Budget Allocation As explained in Section 3.3.2 of the main paper, we use two hyper-parameters, α and β , to adaptively schedule the labeling budgets of the two active selection methods. α is the balance coefficient between density-aware and the uncertainty-based method, and β is

the decay rate of the labeling budgets of the density-aware approach.

For the GTA \rightarrow Cityscapes task, we set $\alpha = 1, \beta = 1$. For the SYNTHIA \rightarrow Cityscapes task, we set $\alpha = 0.5, \beta = 1$. Note that the values of α and β are empirically decided via grid search. The complete analysis of hyper-parameters selection is displayed in Sec. E.

Network Fine-tuning After the active selection step, we acquire ground truth labels of the top-ranked regions in D_T^U and move them to D_T^L . Then, fine-tune the model on $D_S \cup D_T^L$ in a supervised manner. For the fine-tuning step, we utilized the SGD optimizer with the initial learning rate as $2.5e-4$ and the decay rate 0.9. We apply the conventional cross-entropy loss in the fine-tuning step.

Algorithm 1: The pipeline of ADeADA

Input: data pool: $(D_S, D_T = \{D_T^L, D_T^U\})$, where $D_T^L = \emptyset$, hyper-parameters: (α, β)
labeling budget of the k -th active selection round: B^k , number of active selection round: K
Output: the output model h_θ

Warm-up: $h_\theta \leftarrow (D_S, D_T^U, D_T^L)$ according to [40]

for $k \leftarrow 0$ **to** K **do**

 // Construct source and target density estimators

$Z_S, C_S \leftarrow h_\theta(D_S)$

$Z_T, C_T \leftarrow h_\theta(D_T)$

$GMM_{\text{src}} \leftarrow \text{CONSTRUCTGMMs}(Z_S, C_S)$

$GMM_{\text{trg}} \leftarrow \text{CONSTRUCTGMMs}(Z_T, C_T)$

 // Calculate the region importance metric π

$R^* \leftarrow$ a new empty list

for each c **in** $\{1, 2, \dots, C\}$ **do**

$R_c \leftarrow$ Obtain all regions predicted as category c in D_T^U

for each region in R_c **do**

 Obtain the domain density d_S, d_T of each region with GMM_{src} and GMM_{trg}

 Calculate the importance score π according to Eq. 2

end

 Rank all the regions in R_c in descending order based on the important score; then, append it to R^*

 Calculate the categorical KL-divergence $D_{KL}(p_T(z|c) || p_S(z|c))$ according to Eq. 5

end

 // Adaptive Budget Allocation

 Determine B_u^k, B_d^k given (α, β, B^k) according to Eq. 7

 Determine $B_{d,c}$ for each c given the categorical KL-divergence according to Eq. 6

 // Label Acquisition

$S_u^k \leftarrow \text{UNCERTAINTYSELECTION}(B_u^k, h_\theta, D_T^U)$ according to [42]

$S_d^k \leftarrow \text{DENSITYAWARESELECTION}(B_d^k, R^*)$ // Pick top-ranked regions based on the categorical budgets $B_{d,c}$

$X_{\text{active}} \leftarrow S_u^k \cup S_d^k$

$Y_{\text{active}} \leftarrow$ Obtain ground-truth labels from the oracle given X_{active}

$D_T^L \leftarrow D_T^L \cup (X_{\text{active}}, Y_{\text{active}})$

$D_T^U \leftarrow D_T^U \setminus X_{\text{active}}$

 // Supervised fine-tuning

$h_\theta \leftarrow$ Tune the model on $D_S \cup D_T^L$ with cross-entropy loss

end

return h_θ

B. Baseline Active Learning Methods

We describe the implementation of 8 region-based active learning baselines used in our experiments. In the following section, we let R denote a region with N pixels within it, and θ denotes the fixed trained deep learning network.

RAND Randomly select few regions of images in the unlabeled target domain dataset D_T^U for label acquisition.

MAR [42] Wang *et al.* [42] proposed using model softmax margin as the indicator to select informative instances for labeling. Specifically, we produce the score for a region (S_R^{MAR}) by averaging the difference between the two most likely category labels for all pixels within the region, as shown in Eq. 8. After that, we acquire the ground truth labels of few regions with the smallest score, which means the smallest margin, in the unlabeled dataset for each category.

$$S_R^{\text{MAR}} = \frac{1}{N} \sum_{n=1}^N P(\hat{y}_n^1 | R; \theta) - P(\hat{y}_n^2 | R; \theta), \quad (8)$$

where \hat{y}_n^1 is the first most probable label category and \hat{y}_n^2 is the second most probable label category.

CONF [42] The main concept of the confidence selection strategy is to acquire labels for samples whose prediction has the least confidence [42, 44]. As can be observed in Eq. 9, the score for a region (S_R^{CONF}) is produced by averaging the softmax confidence of all pixels within the region. After that, we select a portion of regions with the least confidence score in the unlabeled dataset for label acquisition.

$$S_R^{\text{CONF}} = \frac{1}{N} \sum_{n=1}^N P(\hat{y}_n^1 | R; \theta), \quad (9)$$

where \hat{y}_n^1 is the softmax confidence value of the predicted category label.

ENT [42] In the field of information theory, entropy is a widely used metric to evaluate the information of a probability distribution [33]. The idea of this type of selection strategy is to select regions with the largest entropy for labeling [42]. As shown in Eq. 10, the score for a region (S_R^{ENT}) is formed by averaging the softmax entropy of all pixels in a region. After that, a portion of regions with the largest entropy in the unlabeled dataset is selected for label acquisition.

$$S_R^{\text{ENT}} = -\frac{1}{N} \sum_{n=1}^N \sum_{i=1}^c [P(y_n^i | R; \theta) \cdot \log[P(y_n^i | R; \theta)]], \quad (10)$$

where c is the number of categories, and $P(y_n^i | R; \theta)$ represents the softmax probability that the model predicts pixel n as class i .

BADGE [2] Ash *et al.* proposed selecting a batch of diverse and uncertain samples for labeling with a designed gradient embedding space. Specifically, the method first calculates the gradient embedding of each sample to indicate its uncertainty and then selects diverse samples for label acquisition with k-means++. In our implementation, we produce the regional gradient embedding by averaging the value of all pixels within it. Then, we follow its original implementation to cluster the regions with the k-means++ algorithm.

ReDAL [46] Wu *et al.* proposed acquiring a batch of diverse point cloud regions with high uncertainty for labeling by entropy, 3D characteristics, and greedy diversity selection. In our implementation, we carefully replaced the 3D characteristics term as the 2D edge detection result and followed the rest of the algorithm.

AADA [38] Su *et al.* presented the first active domain adaptation approach for image classification. The concept of this method is to leverage the softmax entropy and the domain discriminator to select uncertain samples that are far from the source domain distribution. In our implementation, we calculated the region-level softmax entropy and domain discriminator result and followed the rest of the algorithm.

CLUE [28] Prabhu *et al.* presented another active domain adaptation method by clustering the uncertainty-weighted embeddings. The same, we treated a region as the fundamental label query unit and followed the original implementation.

C. Proof

We would like to prove Eq.4 in the main paper (line 412).

$$\begin{aligned} D_{\text{KL}}(p_T(c, z) \parallel p_S(c, z)) &= \mathbb{E}_{p_T(c, z)} [\log p_T(c, z) - \log p_S(c, z)] \\ &= \mathbb{E}_{p_T(c, z)} [\log p_T(c) + \log p_T(z|c) - \log p_S(c) - \log p_S(z|c)] \\ &= \mathbb{E}_{p_T(c, z)} [\log p_T(c) - \log p_S(c)] \\ &\quad + \mathbb{E}_{p_T(c, z)} [\log p_T(z|c) - \log p_S(z|c)] \\ &= \mathbb{E}_{p_T(c)} [\log p_T(c) - \log p_S(c)] \\ &\quad + \mathbb{E}_{p_T(c)} [\mathbb{E}_{p_T(z|c)} [\log p_T(z|c) - \log p_S(z|c)]] \\ &= D_{\text{KL}}(p_T(c) \parallel p_S(c)) + \mathbb{E}_{p_T(c)} [D_{\text{KL}}(p_T(z|c) \parallel p_S(z|c))] \end{aligned}$$

D. More Qualitative Results

Due to space limitations, we show more qualitative results in the supplementary material. As shown in Figure 6, we show five inference results of different approaches for the GTA5 \rightarrow Cityscapes domain adaptation task, including success and failure cases.

The first three rows present the results that our method outperforms the UDA method [40] and the previous ADA approach [38]. As can be shown from the picture in the first row, the segmentation result generated by our method creates a clear boundary and is very close to the full supervision, and greatly surpasses the two existing practices. Our method can better capture the structure of the scene and greatly surpasses the two existing practices. The second and the third rows show that our method can better recognize hard categories, such as “train” and “fences” (shown on the red bounding box).

The fourth and fifth rows present two failure cases of our method. As observed from the red bounding boxes, our method performs worse than full supervision in these pictures’ corners or boundary areas. However, compared with the two existing approaches, our method still achieves better results. We believe that the problem of poor performance in the pictures’ corners or boundary areas may be improved through a better active selection strategy, which is worthy of further research in the future.

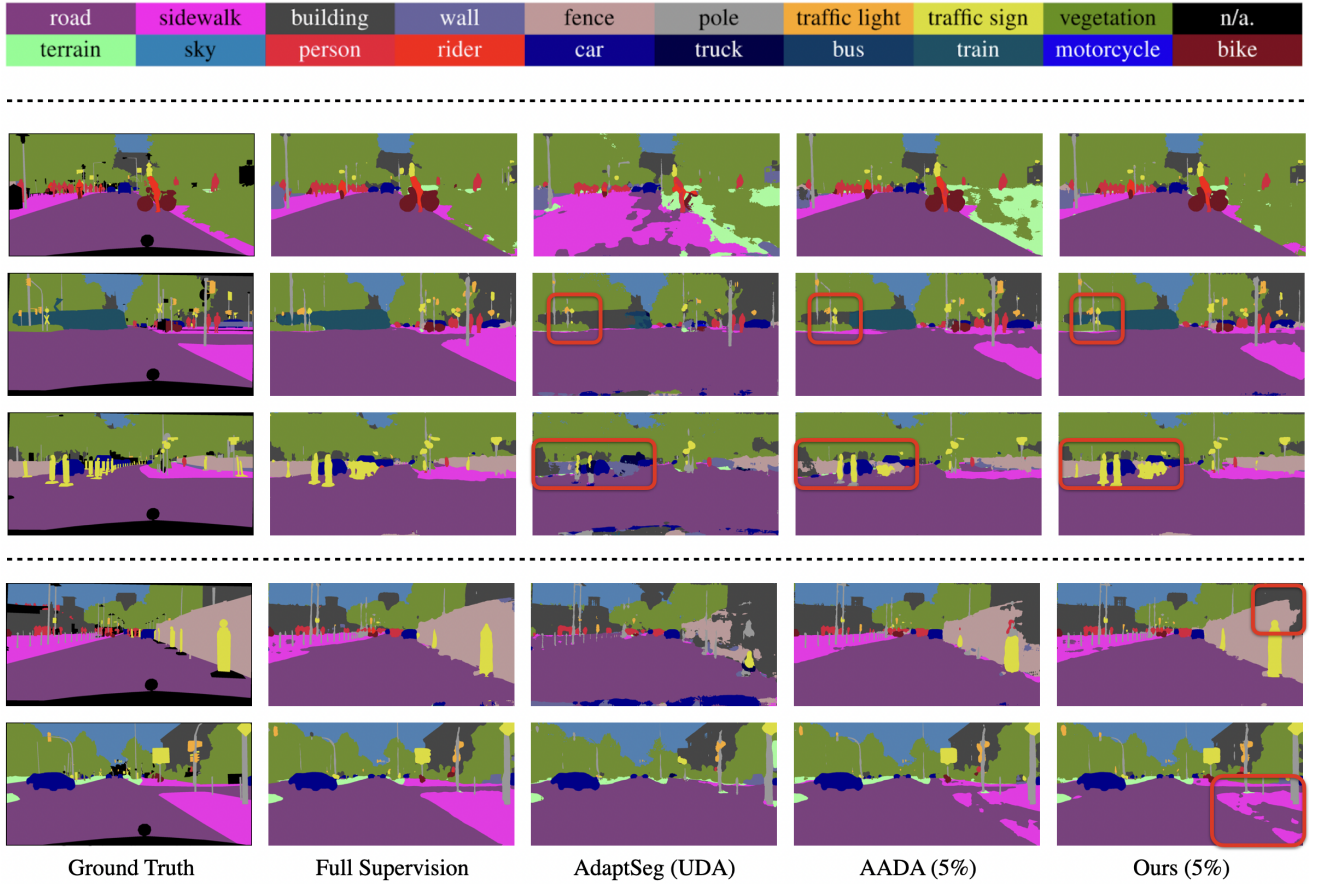


Figure 6. **More Qualitative results of different approaches for the GTA5 \rightarrow Cityscapes domain adaptation task.** We present three success cases (in the top three rows) and two failure cases (in the bottom two rows) of our method. For more detailed explanation, please refer to Sec D.

E. More Experimental Results

Due to space limitations, we show the complete experimental results here. Table 3 reports the performance of the model after the UDA warmup stage. Table 6 and 7 shows the raw data of Figure 3 in the main paper. Table 8 shows the per-class performance of our active learning strategy.

We also conducted comprehensive researches on hyperparameters selection and the robustness of our method. In the following section, we first discuss the effectiveness of two key factors in our dynamic scheduling policy (Section 3.3.2 of the main paper): the selection of the initial balance coefficient and the comparison of different scheduling strategies. Then, we review whether our density-aware method is robust under the inaccurate predicted category, which might happened in the early stages in the ADA (Section 3.2.1 of the main paper).

Effectiveness of Initial Balance Coefficient As mentioned in Section 3.3.2 of the main paper, the balance coefficient α is designed to balance between density-aware and the uncertainty-based method at the first active selection round. We investigate the effectiveness of α with the DeepLabV3+ model backbone for the two tasks.

As can be observed in Table 4, with the aid of partial or full acquired annotations by our designed density-aware method, models are able to obtain higher mIoU scores compared with only using conventional uncertainty-based method ($\alpha = 0$). For the GTA5 \rightarrow Cityscapes task, only adopting density-aware selection strategy at the beginning achieve the best result; while for the SYNTHIA \rightarrow Cityscapes task, choosing $\alpha = 0.5$ to combine density-aware and uncertainty-based methods obtain the best performance. This detailed experimental result confirms the effectiveness of our density-aware selection in severe domain shift.

Effectiveness of Different Scheduling Policies As discussed in Section 3.3.2 of the main paper, due to the rapid domain shift reduction, we design a dynamic scheduling policy to half decay the labeling budget of the density-aware strategy and gradually put more emphasis on the conventional uncertainty-based method. Here we discuss the effectiveness of five different labeling scheduling policies on the GTA5 \rightarrow Cityscapes task with DeepLabV3+ model backbone, including pure uncertainty, pure density, even distribution, linear decay, and half decay.

Even distribution means evenly assigning the labeling budgets to the two methods in every active selection round, which means the proportion of the density-aware selection method is 0.5 for each round. Linear decay refers to the linear decrease of the labeling budgets assigned to the density-aware method. In our implementation, the propor-

tion of density-aware selection method is initialized as 1.0 and linearly decreases by 0.2 as the active selection round increases. Half decay is our proposed scheduling policy described in Section 3.3.2 of the main paper.

As shown in Table 5, adopting our designed half-decay approaches obtain the best performance with the same amount of acquired target annotations.

Influence of Inaccurate Predicted Category As mentioned in Section 3.2.1 in the main paper, our density-aware selection estimates the domain density with the extracted region features and the corresponding predicted categories. Since the predicted category might be inaccurate, especially in the first stage in the ADA, we conducted an experiment to verify whether our method is robust under this issue.

The result shows that indeed the initially predicted category might indeed be inaccurate, but our method can recall more of these mispredicted data for labeling. According to the statistics, about 56% of “target bus regions” were predicted as other classes by the initial model. Still, our method recalled 25% of these mispredicted regions to re-label, while the uncertainty-based methods could only recall 4% of them. Overall, we show our approach is effective even with noisy initial labels in this experiment.

(a) GTA \rightarrow Cityscapes		
	DeepLabV2	DeepLabV3+
mIoU (%)	44.61	45.51
(b) SYNTHIA \rightarrow Cityscapes		
	DeepLabV2	DeepLabV3+
mIoU (%)	39.95	43.04

Table 3. We report the mIoU scores after applying the UDA method [40] as the warmup step. The result shows that the performance of the UDA method is still far from that of full supervision and our method.

(a) GTA \rightarrow Cityscapes with 1% Target Labels					
α	0	0.25	0.5	0.75	1.0
mIoU (%)	59.57	61.95	63.30	63.73	64.03
(b) SYNTHIA \rightarrow Cityscapes with 1% Target Labels					
α	0	0.25	0.5	0.75	1.0
mIoU (%)	61.56	61.98	62.47	62.07	61.87

Table 4. We report the mIoU scores with different balance coefficients α . We found that using only the uncertainty-based method, *i.e.*, $\alpha = 0$, obtained the worst results among all combinations. The results show that using some or all of the obtained annotations through density-aware selection can improve model performance.

Scheduling Policy	mIoU		
	1%	3%	5%
Even Distribution	63.30	69.66	71.15
Linear Decay	64.03	69.49	71.14
Half Decay	64.03	69.86	71.25

Table 5. We compare different label budget scheduling strategies on the GTA \rightarrow Cityscapes task. The result shows that our designed half-decay method performs the best among all strategies.

% Target Labels	RAND	MAR	CONF	ENT	BADGE	ReDAL	AADA	CLUE	ADeADA
1	58.81	57.95	59.90	59.57	62.67	61.97	55.84	60.13	64.03
2	61.11	64.33	65.72	66.08	65.62	65.93	61.71	62.96	67.65
3	62.23	67.08	68.83	68.79	67.73	67.12	64.93	64.99	69.86
4	63.62	68.47	69.55	69.83	68.66	68.55	65.74	65.88	70.66
5	63.50	69.44	70.70	70.70	70.50	68.30	66.01	67.13	71.25

Table 6. Results of mIoU performance (%) on GTA [29] → Cityscapes [10] with DeepLabV3 network backbone.

% Target Labels	RAND	MAR	CONF	ENT	BADGE	ReDAL	AADA	CLUE	ADeADA
1	59.05	60.67	61.94	61.56	61.64	61.08	54.16	60.17	62.47
2	60.96	67.23	68.20	67.75	66.29	66.58	59.84	64.71	69.35
3	63.65	69.68	69.70	70.23	69.18	69.30	63.12	66.50	71.01
4	65.53	70.43	71.17	71.28	70.26	69.97	66.09	67.46	72.40
5	66.09	71.37	71.50	71.76	71.08	71.01	67.03	68.37	72.74

Table 7. Results of 16-classes mIoU performance (%) on SYNTHIA [30] → Cityscapes [10] with DeepLabV3 network backbone.

(a) GTA5 → Cityscapes																					
	% Target Labels	Road	SW	Build	Wall	Fence	Pole	TL	TS	Veg.	Terrain	Sky	PR	Rider	Car	Truck	Bus	Train	Motor	Bike	mIoU
ADeADA (DeepLabV2)	1%	93.63	59.90	86.92	39.59	40.95	44.04	51.78	53.87	88.34	45.30	86.60	71.09	46.82	89.81	57.58	69.71	58.65	52.54	68.45	63.45
	2%	95.34	69.08	88.54	48.24	49.26	45.21	54.41	59.61	89.00	52.73	90.64	73.09	50.23	91.20	69.36	73.00	59.99	56.03	69.57	67.61
	3%	96.11	72.52	88.98	48.33	50.52	46.42	55.35	62.08	89.55	53.86	90.69	74.11	52.69	91.47	67.90	77.01	65.13	59.20	70.75	69.09
	4%	96.27	73.91	89.28	49.03	52.66	47.12	56.44	63.54	89.73	56.52	91.76	74.49	53.74	91.66	68.25	76.29	62.99	59.08	71.21	69.68
	5%	96.29	73.57	89.26	50.01	52.26	47.94	56.91	64.65	89.27	53.94	92.25	73.91	52.86	91.84	69.67	78.87	62.70	57.65	71.05	69.73
ADeADA (DeepLabV3+)	1%	93.19	59.06	87.50	37.95	43.54	45.43	53.63	47.59	88.23	44.72	89.73	72.04	48.58	91.11	63.40	68.98	58.56	54.88	68.47	64.03
	2%	95.50	69.38	88.91	43.63	50.05	48.77	56.19	58.97	89.39	51.66	90.68	73.94	51.31	91.65	66.52	72.15	58.69	57.48	70.40	67.65
	3%	96.27	73.91	89.37	47.65	52.37	50.12	57.14	64.29	89.50	55.64	91.50	75.03	53.03	92.28	69.97	77.16	63.13	57.35	71.54	69.86
	4%	96.77	76.58	89.75	47.28	53.79	52.33	57.92	65.41	89.90	56.69	92.27	75.31	53.01	92.09	68.77	76.43	67.25	58.82	72.16	70.66
	5%	96.97	77.83	89.97	45.98	55.04	52.74	58.69	65.80	90.37	58.94	92.14	75.69	54.36	92.26	69.04	78.01	68.51	59.05	72.33	71.25
(b) SYNTHIA → Cityscapes																					
	% Target Labels	Road	SW	Build	Wall	Fence	Pole	TL	TS	Veg.	Sky	PR	Rider	Car	Bus	Motor	Bike	mIoU	mIoU*		
ADeADA (DeepLabV2)	1%	93.82	61.50	85.21	26.15	19.21	40.75	46.41	53.16	86.11	87.27	70.78	46.77	86.54	34.08	48.49	66.21	59.53	66.64		
	2%	94.95	67.30	87.79	37.92	42.04	44.09	53.45	61.05	88.17	90.11	73.64	53.37	89.98	66.26	53.54	69.36	67.07	73.00		
	3%	95.73	71.75	88.48	38.68	44.08	46.4	54.48	64.64	88.68	90.18	74.49	53.99	90.72	73.27	57.48	70.86	68.99	74.98		
	4%	96.21	73.95	88.93	41.23	48.24	47.45	55.31	65.65	89.23	91.24	74.59	54.39	91.07	73.37	58.21	71.55	70.04	75.67		
	5%	96.41	74.57	89.09	42.51	47.70	47.99	55.64	66.46	89.47	91.73	75.10	55.15	91.37	76.97	57.97	71.77	70.62	76.28		
ADeADA (DeepLabV3+)	1%	92.45	55.44	86.75	34.94	29.07	44.90	48.97	54.43	87.09	90.27	73.66	49.39	88.98	40.74	52.85	69.64	62.47	68.51		
	2%	95.54	71.45	88.78	38.97	45.69	50.34	55.57	64.78	89.46	92.06	75.61	53.38	91.14	69.67	55.49	71.70	69.35	74.97		
	3%	96.13	74.04	89.11	39.64	49.52	52.58	56.24	65.91	89.89	92.80	76.38	54.63	92.20	76.06	58.77	72.31	71.01	76.50		
	4%	96.19	74.40	89.91	48.48	50.71	53.60	58.10	66.88	90.01	93.29	77.15	56.28	92.25	78.39	59.54	73.27	72.40	77.36		
	5%	96.67	76.76	90.27	48.73	51.06	54.24	58.28	67.99	90.41	93.37	77.37	56.41	92.53	77.53	58.88	73.29	72.74	77.67		

Table 8. Complete experimental results of our proposed ADeADA on (a) GTA5 → Cityscapes and (b) SYNTHIA → Cityscapes with different percentage of acquired target labels.